Characterizing Variations in the Ruelle Zeta Function Under Conformal Perturbations to the Metrics of Negatively Curved Riemannian 2-Manifolds

Samanyu Ganesh

Under the direction of

Alain Kangabire
Department of Mathematics
Massachusetts Institute of Technology

Research Science Institute
July 29th, 2025

Abstract

The Ruelle zeta function $\zeta_R(s)$ is a dynamical analog of the Riemann zeta function, defined via the lengths of primitive closed geodesics on a compact Riemannian surface. For negatively curved surfaces, the flow is chaotic and the set of closed orbits is discrete and stable, making $\zeta_R(s)$ well-suited for spectral analysis. In particular, the vanishing order of $\zeta_R(s)$ at $s = 0$ is determined by the Euler characteristic, and its leading coefficient is conjecturally linked to analytic torsion, a spectral invariant of the Laplacian on manifolds. In this paper, we study how that leading coefficient varies under conformal perturbations of the hyperbolic metric of the form $g_\varepsilon = e^{\varepsilon\phi} g_{\mathbb{H}}$. Using recent microlocal techniques developed for resonances of Anosov flows, we reduce the problem to solving the inhomogeneous transport equation $(X+1)(U_- \dot{f}_0) = h$ on the unit cosphere bundle. With explicit expressions for crucial Fourier modes of $\dot{f}_0$ (-1 and 1, specifically), we compute the variation of the zeta function up to second order in ε, offering evidence for the Fried conjecture in new cases.

Summary

This paper explores how certain hidden patterns in the shapes of curved surfaces, like those found in Riemannian geometry and gravitational physics, respond when the surface is slightly changed. We focus on a special function called the Ruelle zeta function, which captures information about how geodesics (the locally-shortest paths that particles, planets, and other phenomena in spacetime naturally follow) loop around on a surface with consistent periods. In particular, we look at how this function's behavior near 0 relates to global geometric properties of the surface. By studying how this behavior changes when the surface's intrinsic metric is gently modified, we gain insight into how local changes affect large-scale spectral (vibrational/wave-like) features.

1 Introduction

The Ruelle zeta function is a dynamical analog of the Riemann zeta function, where the role of prime numbers is instead played by the lengths of primitive closed orbits of a flow. For a compact, oriented Riemannian manifold equipped with a flow φ_t, the Ruelle zeta function is formally defined by

$$\zeta_R(s) = \prod_{\gamma \in G} \big(1 - e^{-s\ell_\gamma}\big),$$

where G is the set of primitive closed orbits and ℓ_γ their periods.

A natural setting for studying this object is the geodesic flow on the unit cosphere bundle of a negatively curved surface. Negative curvature ensures the flow is chaotic: nearby trajectories diverge exponentially, and the primitive closed geodesics are isolated and non-degenerate. These features make the set of closed orbits both rich and discrete, allowing the zeta function to be well-defined and appropriately sensitive to changes in geometry.

In 2016, Dyatlov and Zworski [1] developed a microlocal framework to demonstrate the meromorphic continuation of $\zeta_R(s)$ for general classes of smooth chaotic flows. They later showed that for any oriented, negatively curved surface with Euler characteristic $\chi(\Sigma)$, the function $s^{\chi(\Sigma)}\zeta_R(s)$ is holomorphic and non-vanishing at $s = 0$ [2].

To place this in context, earlier work by Fried [3] had shown that when the metric has constant negative curvature, the zeta function has the precise expansion

$$\zeta_R(s) = \pm(2\pi s)^{\chi(\Sigma)}\big(1 + O(s)\big),$$

connecting the behavior at $s = 0$ directly to a topological invariant. Fried's result is part of a broader conjectural framework that interprets the $\pm 2\pi^{\chi(\Sigma)}$ term (which changes depending on the metric) as proportional to some intgeral power of the *analytic torsion*, a spectral invariant of the Laplacian on a manifold. For example, in the case of constant negative curvature, Medved [4] showed in 2024 that the analytic torsion varies inversely with this leading coefficient, which itself is equal to determinant of a matrix whose entries measure how harmonic differential forms interact with resonance states of the flow.

While the behavior of $\zeta_R(s)$ is well understood in the constant curvature case, much less is known about how it responds to metric deformations. In this paper, we investigate the effect of conformal perturbations of the form

$$g_\varepsilon = e^{\varepsilon\psi}\, g_{\mathbb{H}}, \tag{1}$$

where $g_{\mathbb{H}}$ is the standard hyperbolic metric in the upper half-plane model and φ is a smooth function on the surface. Our goal is to study how the leading coefficient in the expansion

$$\zeta_R(s) = c_\varepsilon\, s^{\chi(\Sigma)} + (\text{higher order terms})$$

depends on ε for compact oriented hyperbolic surfaces.

A central tool in our analysis is the family of 1-forms u_ε arising from Dyatlov and Zworski's microlocal description of resonances in the geodesic flow [2]. These forms admit a decomposition

$$u_\varepsilon = \pi^* \omega_j + df_\varepsilon, \tag{2}$$

where ω_j is a harmonic 1-form on the surface and f_ε is a scalar function capturing the perturbation's contribution to resonance states of the flow. By expanding f_ε in a Taylor series

$$f_\varepsilon = f_0 + \varepsilon \dot{f}_0 + \frac{\varepsilon^2}{2} \ddot{f}_0 + \cdots,$$

we reduce the problem to understanding how the leading and first-order terms in this expansion behave under conformal deformation.

Roadmap. Section 2 introduces a way to construct compact surfaces of negative curvature in a manner that reveals an elegant connection between geodesic flow and contact geometry. In Section 3, we begin by computing f_0 explicitly in order to gain a better understanding of the constant curvature case. Next, we study $\dot{f}_0$, which encodes how the microlocal data changes under perturbation. In particular, Section 4 sees the derivation of a coupled system involving $X\dot{f}_0$ and $U_-\dot{f}_0$. Along the way, we solve the inhomogeneous transport equation $(X+1)(U_-\dot{f}_0) = h$ for $U_-\dot{f}_0$ in terms of the source term h (which itself depends on the perturbation ψ). Finally, in Section 5, we use the paired expressions for $X\dot{f}_0$ and $U_-\dot{f}_0$ to compute the Fourier modes of $\dot{f}_0$ explicitly at frequencies 1 and -1. This step is especially important, because in 2024, Medved [4] showed that all of the the variation in the Ruelle zeta function's leading coefficient c_ε turns out to depend only on these two modes.

2 Preliminaries

2.1 Compact Surfaces of Negative Curvature

Let the surface

$$\mathbb{D} = \{x + yi \in \mathbb{C} : x^2 + y^2 < 1\} \tag{3}$$

denote the Poincaré disk. We equip $\mathbb{D}$ with the following metric:

$$g = \frac{4}{(1-x^2-y^2)^2}(dx^2 + dy^2) = e^{2G(x,y)}(dx^2 + dy^2), \tag{4}$$

where $G(x,y) = \ln 2 - \ln(1-x^2-y^2)$ is implicitly defined. Metrics equipped with conformal factors of the form e^{2G} are especially convenient in that they allow the Gaussian curvature to be expressed

simply and explicity.

Definition 2.1. Let (M, g) be a smooth Riemannian 2-manifold, where the metric takes the isothermal form

$$g = e^{2G(x,y)}(dx^2 + dy^2)$$

for some smooth function G. Then the *Gaussian curvature* K of the surface at each point is given by the expression

$$K = -e^{-2G}\left(\partial_x^2 + \partial_y^2\right) G, \tag{5}$$

a formula from Dyatlov [5] that elegantly encodes how the exponential scaling of lengths warps the underlying geometry.

Example 2.2. It is a classical result the Riemannian 2-manifold $(\mathbb{D}, g)$ defined by (3) and (4) has a constant curvature of -1. Using (5), we see for ourselves that

$$\begin{aligned} K &= -e^{-2G}\left(\partial_x^2 + \partial_y^2\right) G \\ &= -e^{-2G}\left(\frac{2(1+x^2-y^2)}{1-x^2-y^2} + \frac{2(1-x^2+y^2)}{1-x^2-y^2}\right) \\ &= -\frac{(1-x^2-y^2)^2}{4} \cdot \frac{2+2}{(1-x^2-y^2)^2} = -1. \end{aligned}$$

Shifting gears slightly, we turn to another representation of hyperbolic space that is often more amenable to explicit algebraic descriptions.

Definition 2.3. The *hyperbolic plane* $\mathbb{H}$ is the upper half-plane $\{x + iy \in \mathbb{C} : y > 0\}$ equipped with the Riemannian metric $ds^2 = \frac{dx^2+dy^2}{y^2}$.

Remark. The fact that $\mathbb{H}$ also possesses a constant curvature of -1 can be verified by letting $G(x, y) = -\ln y$ in (5).

$\mathbb{H}$'s rich geometric structure admits many symmetries, which can be understood algebraically through the action of certain matrix groups.

Definition 2.4. The projective special linear group $\mathrm{PSL}_2(\mathbb{R}) = \mathrm{SL}_2(\mathbb{R})/\{\pm I\}$ acts on $\mathbb{H}$ by isometries via *Möbius transformations*

$$z \mapsto \frac{az+b}{cz+d},$$

where each transformation is represented by a matrix $\begin{pmatrix} a & b \\ c & d \end{pmatrix} \in \mathrm{SL}_2(\mathbb{R})$ and this action preserves the hyperbolic distance between points.

To build compact surfaces with negative curvature, we next consider discrete subgroups of this isometry group. These subgroups specify exactly which points in the hyperbolic plane should be identified to produce a compact quotient surface.

Definition 2.5. A subgroup $\Gamma \subset \mathrm{PSL}_2(\mathbb{R})$ is called *discrete* if it does not accumulate to the identity; in other words, for any compact set $K \subset \mathbb{H}$, only finitely many $\gamma \in \Gamma$ satisfy $\gamma K \cap K \neq \varnothing$.

Given such a discrete subgroup, the quotient space $S = \Gamma\backslash\mathbb{H}$ is formed by identifying all points lying in the same Γ-orbit. While discreteness ensures that the group action is well-behaved (i.e. properly discontinuous, meaning that small neighborhoods in $\mathbb{H}$ do not get infinitely tangled up under the action of Γ), it does not by itself guarantee that the quotient surface is finite in extent. This construction naturally raises the question of when the resulting quotient surface is compact.

Definition 2.6. A topological space is compact if every open cover has a finite subcover. In our context, *compactness* of the quotient surface $S = \Gamma\backslash\mathbb{H}$ means that S is a finite hyperbolic surface without cusps or boundary.

Remark. The compactness condition on S is equivalent to the requirement that Γ is *cocompact*: that is, there exists a compact subset of $\mathbb{H}$ whose images under the group action cover the upper half-plane in its entirety without overlapping interiors.

This observation motivates the need to understand how one might select a single representative region from which the entire surface can be reconstructed under the group action.

Definition 2.7. A *fundamental domain* for the action of a discrete group Γ on $\mathbb{H}$ is a subset $J \subset \mathbb{H}$ such that every point in $\mathbb{H}$ can be moved into J by applying an element of Γ, and no two such images γD and $\gamma' D$ cover the same point except possibly on the boundary of their closures.

Intuitively, one can think of a fundamental domain as a single "tile" whose edges are identified in pairs under the group action to reconstruct the quotient surface. A particularly useful example of a fundamental domain for this action is the Dirichlet domain centered at a point $p \in \mathbb{H}$.

Definition 2.8. Formally, the *Dirichlet domain* is given by

$$D_p = \{z \in \mathbb{H} : d(z,p) < d(\gamma z, p) \quad \text{for all} \quad \gamma \neq e\}.$$

The Dirichlet domain can be visualized as a geodesic polygon whose sides are pairwise identified by elements of Γ. When Γ contains no elliptic elements (i.e., no elements fixing points of $\mathbb{H}$), the action is free, and S inherits the structure of a smooth hyperbolic surface of constant curvature -1. In this way, one constructs compact oriented surfaces of negative curvature by specifying a discrete group Γ and describing the identifications of edges of a fundamental domain. For a detailed development of this construction, see [6].

Though isometric to $\mathbb{H}$, the Poincaré disk $\mathbb{D}$ lends itself better to the visuzalization hyperbolic surfaces. We now return to $\mathbb{D}$ to illustrate an example of a compact surface with negative curvature constructed via edge identifications.

Example 2.9. The hyperbolic double torus can be realized as the quotient surface $S = \Gamma\backslash\mathbb{D}$, where Γ is a cocompact discrete subgroup of $\mathrm{PSL}_2(\mathbb{R})$ chosen so that its fundamental domain is a regular hyperbolic octagon. Figure 1 shows this Dirichlet domain with edges labeled directionally in pairs; each identification corresponds to a uniquely-determined Möbius transformation, or rather, an element of Γ that acts by isometry. At a specific radius, the sum of interior angles is exactly 2π radians, which is required to produce a smooth genus 2 surface without singularities; this specific hyperbolic double torus is equipped with a metric of constant negative curvature -1.

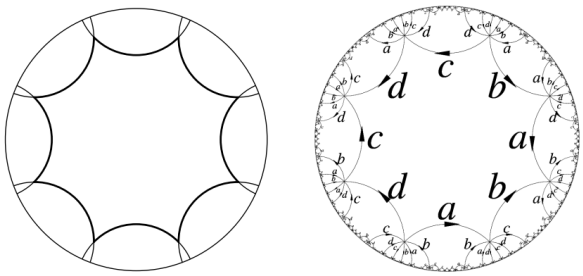

Figure 1: Identification scheme of the hyperbolic double torus as an octagon with side pairings in the hyperbolic plane (taken from [7]).

In negatively curved settings such as Example 2.9, familiar intuitions from Euclidean geometry, especially with regard to notions of parallelism, break down entirely. This fundamental discrepancy sets the stage for our study of geodesics.

2.2 Geodesic Flow in Hyperbolic Space

A tenet of differential geometry is that the concept of a straight line can be generalized to curved spaces by considering paths that look straight when viewed up close through a magnifying glass adapted specifically to the space in which they are embedded.

Definition 2.10. *Geodesics* are curves that locally minimize distance and whose tangent vectors have zero covariant derivative (i.e., the direction of the velocity vector does not twist, turn, or stretch relative to the geometry).

On the sphere, geodesics are great circles; on a flat plane, they are ordinary straight lines.

Example 2.11. Figure 2 shows one way to build generalizable intuition: consider a pilot plotting a route that passes near the poles (such as the path depicted between Los Angeles and Dubai), where distances between longitudes are compressed compared to the equator. This simple fact

[1] `https://aviation.stackexchange.com/questions/90717/why-dont-most-planes-fly-in-a-straight-path`
[2] `http://hyperphysics.phy-astr.gsu.edu/hbase/Relativ/grel.html#c5`

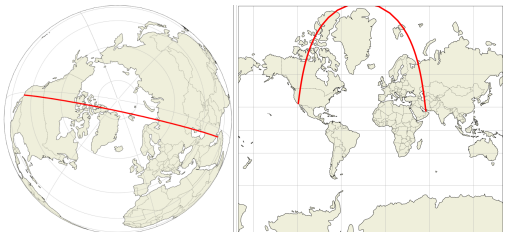

Figure 2: A "curved" flight path between Los Angeles and Dubai.[1]

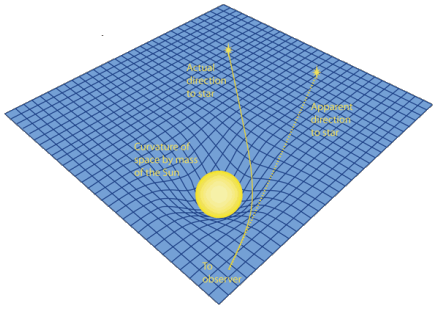

Figure 3: A perturbation to the fabric of spacetime can influence the geometry of geodesics.[2]

about spherical geometry makes "curved paths" (speaking in a Euclidean sense) far more optimal than a straight line between the two cities on a flat projection.

Example 2.12. Alternatively, as shown in Figure 3, the curvature of spacetime around the sun can deflect starlight, so a star hidden behind the sun can still appear visible to us along a curved geodesic.

Similarly to the compression of distances near the poles due to longitudinal lines converging in Example 2.11, in the Poincaré disk, the $1 - x^2 - y^2$ expression in the denominator of the metric means that distances are increasingly stretched near the boundary as $x^2 + y^2$ approaches 1; thus, geodesics veer inward to avoid this stretching. What do geodesics look like in models of hyperbolic space? In $\mathbb{D}$, the short answer is *radial lines* and *circular arcs orthogonal to the disk boundary*, as shown in Figure 4. In $\mathbb{H}$, geodesics are either vertical straight lines or semicircles orthogonal to the real axis.

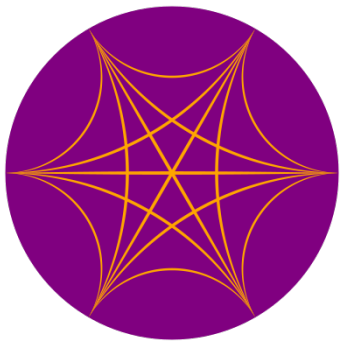

Figure 4: Complete set of geodesics between 6 equally spaced points on the boundary of $\mathbb{D}$

Definition 2.13 (The Long Answer)**.** Just as in Definition 2.1, let (M, g) be a Riemannian surface where the metric takes the conformal form

$$g = e^{2G(x,y)}\,(dx^2 + dy^2),$$

for some smooth function G. Then, as shown in Dyatlov [5], the generator X of the geodesic flow on the unit tangent bundle $S(M)$ is given by

$$X = e^{-G(x,y)}\left(\cos\theta\,\partial_x + \sin\theta\,\partial_y + \left(\cos\theta\,\partial_y G - \sin\theta\,\partial_x G\right)\partial_\theta\right). \tag{6}$$

Although we qualitatively described geodesics in $\mathbb{H}$ as vertical lines or semicircles orthogonal to the x-axis, we now have the tools to formally characterize the infinitesimal behavior of the geodesic flow as a vector field on a surface's unit tangent bundle.

Lemma 2.14. *The generator of the geodesic flow on $S(\mathbb{H})$ with its standard hyperbolic metric is*

$$X = y\left(\cos\theta\,\partial_x + \sin\theta\,\partial_y\right) - \cos\theta\,\partial_\theta. \tag{7}$$

Proof. With conformal factor $G(x, y) = -\ln y$, we substitute into (6) and simplify:

$$\begin{aligned} X &= y\left(\cos\theta\,\partial_x + \sin\theta\,\partial_y\right) + \left(\cos\theta\left(-\tfrac{1}{y}\right) - \sin\theta\,(0)\right)\partial_\theta \\ &= y\left(\cos\theta\,\partial_x + \sin\theta\,\partial_y\right) - \cos\theta\,\partial_\theta. \end{aligned}$$

■

Remark. Through an analogous computation, we can arrive at the following dynamical system in (x, y, θ) that describes the geodesic flow in $\mathbb{D}$: $\dot{x} = \frac{1-r^2}{2}\cos\theta$, $\dot{y} = \frac{1-r^2}{2}\sin\theta$, and $\dot{\theta} = \frac{2}{1-r^2}(x\sin\theta - y\cos\theta)$, where $r^2 = x^2 + y^2$ and the dot notation indicates differentiation with respect to time.

The geodesic flow lies within the scope of a conjectural framework proposed by Fried [3], which asserts that for certain vector fields on compact hyperbolic manifolds,

$$\zeta_R(0) \propto T(M)^r, \tag{8}$$

where r depends on the flow's induced action on twisted cohomology and $T(M)$ denotes the Ray–Singer analytic torsion associated with the underlying manifold and vector bundle structure.

Remark. We do not define Ray–Singer analytic torsion explicitly, since, as outlined in the introduction, our approach centers instead on the Fourier-analytic description of resonance states of the geodesic flow. It nonetheless remains helpful to keep in mind its appearance as a spectral bridge between dynamics and topology, even as our focus shifts to the microlocal level.

In 1986, Fried [3] proved his conjecture for compact surfaces of constant negative curvature, resulting in an inverse relationship defined by $r = -1$ in (8). This class of surfaces includes precisely

the smooth hyperbolic double torus described in the preceding section. Intuition can be built by visualizing the geodesic flow on this surface.

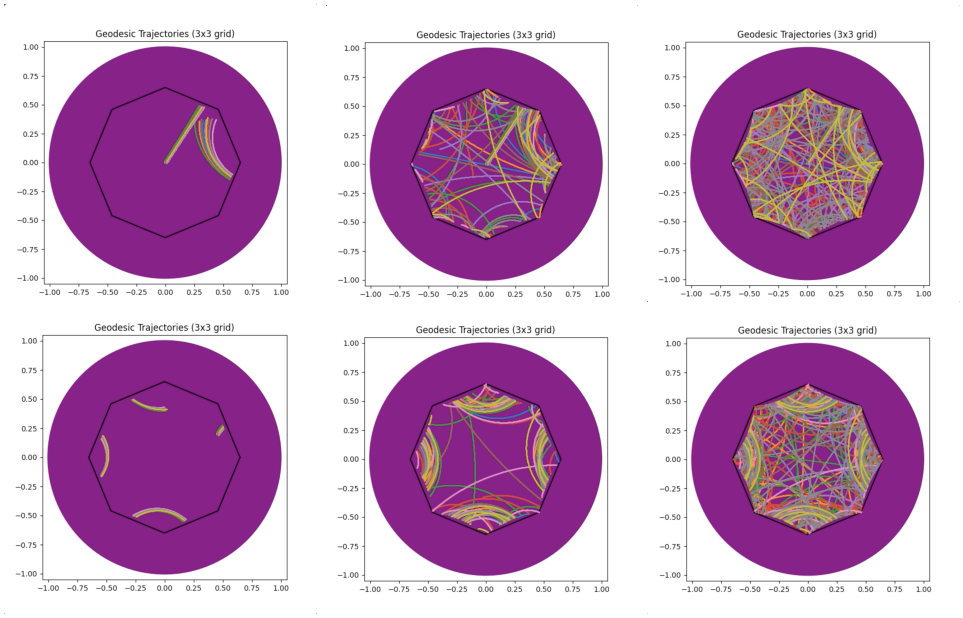

Figure 5: Visualization of divergence of tangent vectors under the geodesic flow on the hyperbolic double torus at times $t = 3, 18, 72$ (step size of 0.01). Each image shows a 3×3 grid of points spaced 0.1 units apart around the origin (top row) and the point $(0.45, 0.2)$ (bottom row), all with an initial direction of 1 radian with respect to the horizontal.

The top row in Figure 5 corresponds to one set of initial conditions, while the bottom row corresponds to another. The visualizations in Figure 5 were generated by approximating solutions to the system of differential equations present in the above remark with a time step of 0.01.

The divergence of nearby trajectories observed in these images stems directly from the constant negative curvature of the hyperbolic double torus. This property ensures uniform hyperbolicity of the geodesic flow, making it a classic example of an Anosov flow.

Definition 2.15. A flow $\varphi^t : TM \to TM$ is called *Anosov* if its tangent space at every point in the tangent bundle splits continuously into stable, unstable, and flow directions, with the stable and unstable directions exhibiting uniform exponential contraction and expansion under the flow.

This hyperbolic behavior is a hallmark of chaotic dynamics and is strongly connected to the negative curvature of the underlying manifold. The fact that the orbits of an Anosov flow are dense in the unit tangent bundle ensures that the dynamical Ruelle zeta function reflects the global geometry and topology of the manifold, providing the necessary link to spectral invariants that Fried's conjecture depends on.

To formallly characterize the behavior of geodesics in hyperbolic space, we describe the geometry

of the unit tangent bundle $S(M)$ and introduce a natural frame adapted to the geodesic flow.

Definition 2.16. Let (M, g) be a Riemannian surface with conformal metric $g = e^{2G(x,y)}(dx^2+dy^2)$. Let X be defined as in Definition 2.13. Then the following vector fields are defined on the unit tangent bundle $S(M)$:

$$\begin{aligned} V &= \partial_\theta, \\ X_\perp &= [X, V], \\ U_\pm &= X_\perp \pm V, \text{ and} \\ \eta_\pm &= \tfrac{1}{2}(X \pm iX_\perp). \end{aligned}$$

Dyatlov [5] notes that together, X, $X_\perp$, and V form a natural local frame for the tangent bundle of $S(M)$. Let $[A, B] = AB - BA$ denote the commutator of operators A and B. The relations

$$[X, V] = X_\perp, \quad [X_\perp, V] = -X, \text{ and } [X, X_\perp] = -KV, \tag{9}$$

where K is the Gaussian curvature in accordance Definition 2.1), also serve to illuminate the symmetries and structure of the flow.

As an exercise, we derive an explicit formula for $X_\perp = [X, V]$ in the case of the upper half plane $\mathbb{H}$ equipped with the metric $g = \frac{dx^2+dy^2}{y^2}$.

Lemma 2.17. *Let $M = \mathbb{H}$ with standard conformal factor $G(x, y) = -\ln y$. Then the orthogonal vector field $X_\perp = [X, V]$ takes the form*

$$X_\perp = y\,(\sin\theta\,\partial_x - \cos\theta\,\partial_y) + \sin\theta\,\partial_\theta.$$

Proof. Substitute $G(x, y) = -\ln y$ into Definitions 2.13 and 2.16, use the expressions for X and V, and compute

$$X_\perp = [X, V] = XV - VX = -\partial_\theta X,$$

Differentiating X with respect to θ and taking its additive inverse yields the desired result. ∎

The local frame $\{X, X_\perp, V\}$ for the tangent bundle $T(S(M))$ captures the natural geometric motions of the geodesic flow: forward movement, orthogonal deviation, and fiber rotation.

However, it follows immediately from the expressions for $U_\pm$ in Definition 2.16 that the collection $\{X, U_+, U_-\}$ also forms a local frame for $T(S(M))$. According to Dyatlov [8], this spanning set is particularly natural from a dynamical point of view as it produces the unstable and stable bundles associated with the Anosov splitting. In fact, one can revise Definition 2.15 to say that the stable and unstable bundles are locally generated by U_- and U_+, respectively.

This perspective invites a shift to a viewpoint in which the cotangent bundle and its associated

1-forms become the tools of choice for studying generalized functions (resonant states) that remain unchanged along the flow.

2.3 The Dual Frame, Cotangent Bundle, and Contact Forms

To analyze distributions and resonances associated with the flow, it is often more convenient to work in the dual picture, a thought that brings us to a discussion of the cotangent bundle on Riemannian surfaces. In this setting, the dual frame consists of the canonical 1-form α, along with U_-^* and U_+^*, which annihilate the stable and unstable directions, respectively.

Before we proceed, it is useful to establish key algebraic relations between the vector fields that generate our local frame.

Lemma 2.18. *The operators X and $U_\pm$ satisfy the commutation relations*

$$[X, U_\pm] = \pm U_\pm. \tag{10}$$

Proof. Recall from Definition 2.16 that $U_\pm = X_\perp \pm V$. Using linearity property of Lie brackets, we expand as follows:

$$[X, U_\pm] = [X, X_\perp \pm V] = [X, X_\perp] \pm [X, V].$$

By way of the relations present in (9), we find that $[X, U_\pm] = -KV \pm X_\perp = V \pm X_\perp = U_\pm$, as claimed. The last two steps followed from Lemma 2.2 and Defintion 2.16, respectively. ∎

We now turn to the dual frame $\{\alpha, U_-^*, U_+^*\}$ in the *unit cotangent bundle* $T^*(S(M))$, which naturally pairs with the vector fields $\{X, U_+, U_-\} \subset T(S(M))$. Among these, the form α plays a distinguished role, as it encodes the geometric information of the geodesic flow in a way that is intrinsic to the surface.

Definition 2.19. The *canonical 1-form* α (also known as the *contact form*) is defined smoothly and pointwise by

$$\alpha_x(v) := \langle d\pi(v), x \rangle,$$

where $x \in S(M) \subset TM$, $v \in T_x(S(M))$, $\pi : S(M) \to M$ is the natural projection, and α_x denotes a covector in the fiber $T_x^*(S(M))$. In other words, α evaluates a tangent vector v on the base manifold by projecting it down and pairing it with the unit tangent vector x itself.

This 1-form α satisfies a number of important properties. First, it defines a *contact structure* on the unit tangent bundle of a 2-manifold, which can be viewed on its own as a 3-manifold. In particular, the wedge product

$$d\mathrm{vol}_\alpha = \alpha \wedge d\alpha$$

is a nowhere-vanishing 3-form on $S(M)$, and thus determines both an orientation and a natural volume form on the manifold. Contact geometry enters the picture precisely at this point by equipping $S(M)$ with a geometric structure that interacts richly and understandably with the geodesic flow.

Remark. In particular, the geodesic flow on a compact Riemannian surface is incompressible in the sense that, as the system evolves under the flow, no volume in phase space is created or destroyed.

Definition 2.20. Let $\alpha \in \Omega^1(S(M))$ be a contact form. The unique vector field X on S(M) satisfying

$$\iota_X \alpha = \alpha(X) = 1, \qquad \iota_X d\alpha = d\alpha(X) = 0 \tag{11}$$

is called the *Reeb vector field* associated to α.

Dyatlov and Zworski [2] write that the condition of a non-vanishing volume form $d\mathrm{vol}_\alpha$ also implies the *uniqueness* of the Reeb flow. These defining relations also appear in [8, Definition 2.2], which further relates that the geodesic flow on a Riemannian surface is a prototypical example of a Reeb flow. The form α defines the direction of motion on the surface, and the geodesic vector field X is characterized precisely by the identities in (11). The first identity, $\iota_X \alpha = 1$, asserts that the geodesic vector field flows in the direction picked out by the unit tangent vector at each point. The second identity, $\iota_X d\alpha = 0$, encodes the fact that the flow preserves the contact structure—that is, the 2-plane distribution defined by $\ker(\alpha)$ is invariant under the infinitesimal action of X.

We now turn to the remaining elements of the dual frame. Since U_+ and U_- span the unstable and stable bundles, respectively, we define their duals as follows.

Definition 2.21. Let $\{X, U_+, U_-\}$ be a local frame on $T(S(M))$. The *dual coframe* $\{\alpha\,, U_-^*, U_+^*\} \subset T^*(S(M))$ is the unique set of 1-forms satisfying

$$\alpha(X) = 1, \quad \alpha(U_\pm) = 0; \qquad U_\pm^*(U_\mp) = 1, \quad U_\pm^*(X) = U_\pm^*(U_\pm) = 0.$$

Thus, U_+^* and U_-^* project onto the stable and unstable directions and vanish on the flow direction. These dual objects are particularly important in the microlocal analysis of Pollicott–Ruelle resonances and the construction of anisotropic Sobolev spaces, as seen in the work of Dyatlov [8].

This dual perspective, grounded in contact geometry, will serve as a foundation for our study of the microlocal structure of resonant states and the spectral properties of the geodesic flow.

We now recall a basic structural property of the resonant 1-forms u_ε defined in (2). As shown in Dyatlov–Zworski [2, Proposition 3.1], any distributional 1-form of the form $u_\varepsilon = \pi^*\omega_j + df_\varepsilon$ satisfying the resonance condition at zero must also obey

$$\iota_{X_\varepsilon} u_\varepsilon = 0. \tag{12}$$

Since our main interest is in how these forms change under perturbation, we will frequently differentiate (12) with respect to ε near 0. To facilitate such computations and clarify notation, we adopt the following conventions:

- $X := X_0$ and $\alpha := \alpha_0$ denote the unperturbed geodesic vector field and contact form, respectively;
- $\dot{f}_0$ denotes $\frac{d}{d\varepsilon} f_\varepsilon \big|_{\varepsilon=0}$.

Example 2.22. With the aforementioned notation in mind, it can be illustratively shown that the contact form α_ε dual to X_ε satisfies

$$\dot{\alpha}_\varepsilon = \psi\, e^{\varepsilon\psi} \alpha_\varepsilon, \text{ so in particular } \dot{\alpha}_0 = \psi\alpha.$$

This result follows from the fact that conformal perturbation of the metric rescales the contact form by $e^{\varepsilon\psi}$, and differentiation in ε yields the stated formula.

3 A minor extension of results on the zeroth-order term

Let X and $\eta_\pm$ be defined as in Definitions 2.13 and 2.16. In 2024, Medved [4] showed that $\{f_0^{(k)}\}$ satisfy the recurrence relations

$$k\, f_0^{(k)} = -2\,\eta_+\, f_0^{(k-1)} = +2\,\eta_-\, f_0^{(k+1)} \tag{13}$$

for all integers k, together with the conditions $f_0^{(1)} = 2\,X\big(\pi^*\,\psi\big)$ and $\eta_-\, f_0^{(0)} = 0$.

Medved [4] computed only the modes $f_0^{(\pm 1)}$, as her Lemma 3.3 showed that all other modes vanish when integrated against the 2-form defining analytic torsion. In this section, we extend her computation by solving the full recurrence explicitly, yielding a closed-form expression for all higher non-vanishing modes.

Lemma 3.1. *For all integers $k \geq 1$,*

$$f_0^{(k)} = (-1)^{k-1}\, \frac{2^{k-1}}{k!}\, \eta_+^{k-1} \big[\, 2\, X(\pi^*\,\psi)\big],$$

and $f_0^{(k)} = 0$ for all $k \leq 0$.

Proof. We proceed by induction.
Positive modes: For $k = 1$, the formula holds by definition. Assuming it holds for k, applying (13) gives

$$f_0^{(k+1)} = -\frac{2}{k+1}\eta_+ f_0^{(k)} = (-1)^k \frac{2^k}{(k+1)!}\eta_+^k \big[2X(\pi^*\psi)\big],$$

which completes the inductive step.
Negative modes: Starting with $\eta_- f_0^{(0)} = 0$ and proceeding by a downward recurrence using (13) (specifically, $k f_0^{(k)} = 2\eta_- f_0^{(k+1)}$) clearly proves the stated result for all of the negative modes. ■

4 Solving for $X\dot{f}_0$ and $U_-\dot{f}_0$

Our first main result, Theorem 4.2, relies heavily on the machinery of Section 2.3. Before stating the theorem, we establish a key relation between the 1-forms comprising the basis of the dual frame.

Lemma 4.1. *The exterior derivative of the canonical 1-form α_0 from Definition 2.19 on $S(M)$ satisfies*

$$d\alpha_0 = 2\,U_+^* \wedge U_-^*,$$

where U_+^* and U_-^* are dual to U_+ and U_-, respectively.

Proof. For an arbitrary 1-form β and vector fields A and B, it is known that $d\beta(A,B) = A(\beta(B)) - B(\beta(A)) - \beta([A,B])$. We apply this fact with $\beta = \alpha_0$, also making use of $\alpha_0(X) = 1$ and $\alpha_0(U_\pm) = 0$ as given in Definition 2.21. We first evaluate

$$d\alpha_0(X, U_\pm) = X[\alpha_0(U_\pm)] - U_\pm[\alpha_0(X)] - \alpha_0([X, U_\pm]) = 0 - U_\pm(1) - \alpha_0(\pm U_\pm) = 0.$$

Here, Lemma 2.18 was used to evaluate $[X, U_\pm]$.

Next, we compute $d\alpha_0(U_+, U_-) = U_+[\alpha_0(U_-)] - U_-[\alpha_0(U_+)] - \alpha_0([U_+, U_-]) = -\alpha_0([U_+, U_-]) = -\alpha_0([X_\perp + V, X_\perp - V]) = -\alpha_0([X_\perp, X_\perp] - [X_\perp, V] + [V, X_\perp] - [V, V])$. By the commutator relations from (9),

$$d\alpha_0(U_+, U_-) = -\alpha_0(0 - (-X) + X - 0) = -2 \cdot \alpha_0(X) = -2.$$

Since $d\alpha_0$ vanishes on $(X, U_\pm)$ and is skew-symmetric, it must therefore be a multiple of $U_+^* \wedge U_-^*$. We let $d\alpha_0 = c\,U_+^* \wedge U_-^*$. To determine the coefficient, we apply both sides to (U_+, U_-):

$$\begin{aligned} -2 = d\alpha_0(U_+, U_-) = c \cdot (U_+^* \wedge U_-^*)(U_+, U_-) &= c \cdot (U_+^*(U_+)U_-^*(U_-) - U_+^*(U_-)U_-^*(U_+)) \\ &= c \cdot (0 - 1 \cdot 1) = -c, \end{aligned}$$

so $c = 2$ and the proof is complete. ■

We are now ready to solve explicitly for $X\dot{f}_0$.

Theorem 4.2. $X\dot{f}_0 = (X_\perp \pi^* \psi)\,(V f_0)$.

Proof. Taking the derivative at $\varepsilon = 0$ on both sides of (12), we obtain

$$0 = \dot{\imath}_0(X_0) + u_0(\dot{X}_0) = d\dot{f}_0(X_0) + u_0(\dot{X}_0) = X_0(\dot{f}_0) + u_0(\dot{X}_0), \tag{14}$$

and thus solving for $X\dot{f}_0$ is equivalent to computing the expression $-u_0(\dot{X}_0)$. Note that $\dot{u_0} = d\dot{f}_0$, since the harmonic 1-forms present in the definition of the resonance states u_ε do not depend on ε.

We now shift our focus to computing $\dot{X}_0$. Recall that by the decomposition of vector fields on $S(M)$ into the framing $\{X, U_+, U_-\}$, any vector field may be written as $\dot{X}_0 = a\,X + b\,U_+ + c\,U_-$ for scalar functions $a, b, c \in C^\infty(S(M))$. Furthermore, by the relations in Definition 2.21, the coefficients can be gleaned by pairing $\dot{X}_0$ with the operators that comprise the dual coframe:

$$(a,\, b,\, c) = (\alpha(\dot{X}_0),\, U_-^*(\dot{X}_0),\, U_+^*(\dot{X}_0)).$$

To proceed, we differentiate (again at $\varepsilon = 0$) the two conditions that characterize Reeb vector fields in Definition 2.20:

$$\iota_X(\alpha) = 1 \quad \Longrightarrow \quad \dot{\alpha_0}(X_0) + \alpha_0(\dot{X}_0) = 0, \tag{15}$$

$$\iota_X(d\alpha) = 0 \quad \Longrightarrow \quad \iota_{\dot{X}_0}(d\alpha_0) + \iota_{X_0}(d\dot{\alpha_0}) = 0. \tag{16}$$

Consequently, notice that (15) allows us to compute $a = \alpha_0(\dot{X}_0) = -\dot{\alpha_0}(X_0) = -(\pi^*\,\psi)\cdot\alpha_0(X_0) = -(\pi^*\,\psi)\cdot\iota_{X_0}\alpha_0 = -(\pi^*\,\psi)$. The appearance of $\pi^*\,\psi$ here (and throughout the proof) is due to the fact that ψ is a function on the base manifold (no direction specified), and thus we must pull it back to $S(M)$ in order to consistently apply it to vector fields and differential forms defined on the unit tangent bundle. Additionally, notice that the logic of Example 2.22 was used in substituting for $\dot{\alpha_0}$ in the computation above.

To compute the remaining scalar functions b and c, we first use (16) to see that

$$\begin{aligned}
\iota_{\dot{X}_0}(d\alpha_0) &= -\iota_{X_0}(d\dot{\alpha_0}) \\
&= -\iota_X\left(d((\pi^*\,\psi)\,\alpha_0)\right) \\
&= -\iota_X\left(d(\pi^*\,\psi)\wedge\alpha_0 + (\pi^*\,\psi)\,d\alpha_0\right) \\
&= -\left(\iota_X(d(\pi^*\,\psi)\wedge\alpha_0) + (\pi^*\,\psi)\,\iota_X(d\alpha_0)\right) \\
&= -\left(d(\pi^*\,\psi)(X)\,\alpha_0 - \alpha_0(X)\,d(\pi^*\,\psi) + (\pi^*\,\psi)\cdot 0\right) \\
&= d(\pi^*\,\psi) - (X\,\pi^*\,\psi)\,\alpha_0.
\end{aligned}$$

On the other hand, Lemma 4.1 allows us to expand as follows:

$$\iota_{\dot{X}_0}(d\alpha_0) = 2\big(U_+^*(\dot{X}_0)\,U_-^* - U_-^*(\dot{X}_0)\,U_+^*\big) = 2(c\,U_-^* - b\,U_+^*).$$

Then, equating both expressions for $\iota_{\dot{X}_0}(d\alpha_0)$, we get

$$2(c\,U_-^* - b\,U_+^*) = d(\pi^*\,\psi) - (X\,\pi^*\,\psi)\,\alpha_0.$$

Now apply both sides to U_- and U_+, remembering that $\alpha_0(U_\pm) = 0$:

$$-2b = d(\pi^*\psi)(U_-) \implies b = -\tfrac{1}{2}d(\pi^*\psi)(U_-); \quad 2c = d(\pi^*\psi)(U_+) \implies c = \tfrac{1}{2}d(\pi^*\psi)(U_+).$$

Putting it all together, we have

$$\begin{aligned}
\dot{X}_0 &= -(\pi^*\psi)\,X - \frac{1}{2}d(\pi^*\psi)(U_-)\,U_+ + \frac{1}{2}d(\pi^*\psi)(U_+)\,U_- \\
&= -(\pi^*\psi)\,X - \frac{1}{2}d(\pi^*\psi)(X_\perp - V)\,(X_\perp + V) + \frac{1}{2}d(\pi^*\psi)(X_\perp + V)\,(X_\perp - V) \\
&= -(\pi^*\psi)\,X - \frac{1}{2}\big(X_\perp(\pi^*\psi) - V(\pi^*\psi)\big)\,(X_\perp + V) + \frac{1}{2}\big(X_\perp(\pi^*\psi) + V(\pi^*\psi)\big)\,(X_\perp - V) \\
&= -(\pi^*\psi)\,X - X_\perp(\pi^*\psi)(V) + V(\pi^*\psi)(X_\perp) \\
&= -(\pi^*\psi)\,X - X_\perp(\pi^*\psi)(V).
\end{aligned}$$

To finish, we use (14) to compute

$$\begin{aligned}
X_0\dot{f}_0 = -u_0(\dot{X}_0) &= -u_0\big(-(\pi^*\psi)\,X - X_\perp(\pi^*\psi)(V)\big) \\
&= u_0\big((\pi^*\psi)\,X\big) + u_0\big(X_\perp(\pi^*\psi)(V)\big) \\
&= (\pi^*\psi)\,X(u_0) + (X_\perp\,\pi^*\psi)(Vf_0) \\
&= (X_\perp\,\pi^*\psi)(Vf_0),
\end{aligned}$$

where the last step follows from (12), since $X(u_0) = \iota_X u = 0$. ∎

Having established the behavior and properties of $\dot{f}_0$ under the operator X, we now turn to a key technical lemma that will facilitate the extension of these results to related vector fields in $T(S(M))$.

Lemma 4.3. *Define $\bar{f} = U_-\dot{f}_0$ and let X be as in Definition 2.13 with $G = \ln y$. Furthermore, let $h(x, y, \theta)$ be given. Then the general solution $\bar{f}(x, y, \theta)$ to the partial differential equation*

$$(X + 1)\bar{f} = h$$

can be expressed as

$$\bar{f}(x, y, \theta) = e^{-s}\int_0^s e^\sigma\, h\left(\frac{2y_0}{e^{-2\sigma}+1} + x_0 - y_0, \quad \frac{2y_0e^{-\sigma}}{e^{-2\sigma}+1}, \quad 2\tan^{-1}(e^{-\sigma}) - \frac{\pi}{2}\right)d\sigma + \bar{f}(0),$$

where $(x_0, y_0, s) = \big(y\tan\theta + x,\, y\sec\theta,\, -\ln\big|\tan\big(\frac{\theta}{2} + \frac{\pi}{4}\big)\big|\big)$.

Proof. We solve the inhomogeneous PDE by the method of characteristics. Introduce the parameter

s along characteristic curves (geodesic paths). The resulting system is

$$\frac{dx}{ds} = y\cos\theta, \quad \frac{dy}{ds} = y\sin\theta, \quad \frac{d\theta}{ds} = -\cos\theta.$$

Step 1: Solve for $\theta(s)$. Integrating both sides of $\frac{d\theta}{ds} = -\cos\theta$ yields

$$\int \sec\theta\, d\theta = -\int ds \quad \Longrightarrow \quad \ln|\sec\theta + \tan\theta| = -s + C_\theta \quad \Longrightarrow \quad \ln\left|\tan\left(\frac{\theta}{2} + \frac{\pi}{4}\right)\right| = -s + C_\theta.$$

Applying the initial condition $\theta(0) = 0$, we get that $\ln\left|\tan\left(\frac{0}{2} + \frac{\pi}{4}\right)\right| = 0 + C_\theta$, and so $C_\theta = \ln 1 = 0$. Therefore,

$$s = -\ln\left|\tan\left(\frac{\theta}{2} + \frac{\pi}{4}\right)\right| \quad \Longrightarrow \quad \theta(s) = 2\tan^{-1}\left(e^{-s}\right) - \frac{\pi}{2}.$$

Step 2: Solve for $y(s)$. Separate variables and integrate:

$$\frac{dy}{ds} = y\sin\theta(s) \quad \Longrightarrow \quad \frac{1}{y}\,dy = \sin\theta(s)\,ds \quad \Longrightarrow \quad \ln y = \int \sin\left(2\tan^{-1}(e^{-s}) - \frac{\pi}{2}\right)\,ds.$$

Using the identity $\sin(\phi - \frac{\pi}{2}) = -\cos\phi$, we obtain

$$\ln y = -\int \cos\left(2\tan^{-1}(e^{-s})\right)\,ds = \int \left(1 - 2\cos^2\left(\tan^{-1}(e^{-s})\right)\right)\,ds,$$

Next, imagining a right triangle with legs of length 1 and e^{-s} and a hypotenuse of length $\sqrt{1+e^{-2s}}$, we can simplify $\cos^2\left(\tan^{-1}(e^{-s})\right)$ as $\left(\frac{1}{\sqrt{1+e^{-2s}}}\right)^2 = \frac{1}{1+e^{-2s}}$, which implies that

$$\ln y = \int \left(1 - \frac{2}{1+e^{-2s}}\right) = \int \frac{e^{-2s}-1}{e^{-2s}+1}\,ds = -s - \ln(1+e^{-2s}) + C_\theta.$$

We now have $y = e^{C_\theta} \cdot \frac{e^{-s}}{1+e^{-2s}}$. Apply the initial condition $y(0) = y_0$:

$$y_0 = e^C \cdot \frac{1}{1+1} = \frac{e^C}{2} \quad \Longrightarrow \quad e^C = 2y_0.$$

Hence, $y(s) = 2y_0 \cdot \frac{e^{-s}}{1+e^{-2s}}$.

Step 3: Solve for $x(s)$. We begin with

$$\frac{dx}{ds} = y(s)\cos\theta(s) = \frac{2y_0 e^{-s}}{1+e^{-2s}} \cdot \sin\left(2\tan^{-1}(e^{-s})\right).$$

Using a similar visualization of a right triangle with legs of length 1 and e^{-s}, we arrive at the fact that $\sin(2\tan^{-1} x) = \frac{2x}{1+x^2}$. Employing this identity with $x = e^{-s}$, we see that

$$\frac{dx}{ds} = \frac{2y_0 e^{-s}}{1+e^{-2s}} \cdot \frac{2e^{-s}}{1+e^{-2s}} = \frac{4y_0 e^{-2s}}{(1+e^{-2s})^2} \quad \Longrightarrow \quad x(s) = \int \frac{4y_0 e^{-2s}}{(1+e^{-2s})^2} ds.$$

Let $u = e^{-2s} + 1$, so $du = -2e^{-2s}ds$ and $ds = -\frac{du}{2u}$. Rewrite the integral:

$$x(s) = \int \frac{4y_0 u}{u^2}\left(-\frac{du}{2u}\right) = -2y_0 \int \frac{1}{u^2} du = 2y_0 \frac{1}{u} + C_x,$$

so

$$x(s) = \frac{2y_0}{1+e^{-2s}} + C_x.$$

Apply the initial condition $x(0) = x_0$ to get that $C_x = x_0 - y_0$, which means that $x(s) = \frac{2y_0}{e^{-2s}+1} + x_0 - y_0$.

Step 4: Solve the PDE along characteristics. Along characteristic curves, define

$$\bar{f}(s) := \bar{f}(x(s), y(s), \theta(s)).$$

Then the PDE $(X+1)\bar{f} = h$ reduces to the ODE

$$\frac{d}{ds}\bar{f}(s) + \bar{f}(s) = h(x(s), y(s), \theta(s)).$$

Multiplying through by the integrating factor e^s simply yields $\frac{d}{ds}\big(e^s \bar{f}(s)\big) = e^s h(x(s), y(s), \theta(s))$. Integrate from 0 to s to finish:

$$e^s \bar{f}(s) - \bar{f}(0) = \int_0^s e^\sigma h(x(\sigma), y(\sigma), \theta(\sigma)) d\sigma.$$

Substitute the explicit characteristic formulas for $x(\sigma), y(\sigma), \theta(\sigma)$ to get the formula in the lemma statement.

To see where the expressions for x_0, y_0, and s come from, notice that each point (x, y, θ) in the unit tangent bundle determines a unique oriented geodesic in $\mathbb{H}$—or in other words, determines a unique semicircle orthogonal to the x-axis. The initial conditions (x_0, y_0) is chosen as the highest point on that semicircle (its "tip") -and s measures hyperbolic arc-length from this tip along the geodesic. Intuitively, the value of s is determined solely by θ, since the orientation θ at any point along the geodesic fixes how far along the semicircle one must go to reach the tip. In this way, $(x_0, y_0) = (y\tan\theta + x,\, y\sec\theta)$ follows from elementary coordinate geometry. This ordered pairsimply records the Euclidean coordinates of the semicircle's top point, from which s then measures hyperbolic distance. ■

This parameterization clarifies the geometry underlying the flow. However, in order to track how a particle would have moved along its past trajectory, we shift the domain of integration from $[0,\, s]$ to $(-\infty,\, 0]$, effectively allowing the system's history to unfold naturally along the backwards flow without relying on an external parameter.

Definition 4.4. Formally, we reparameterize by defining the *flow map* φ_t for $t \leq 0$ as

$$\varphi_t(x, y, \theta) = \left(\frac{2y_0}{1 + e^{-2t}} + x_0 - y_0,\, \frac{2y_0 e^{-t}}{1 + e^{-2t}},\, 2\tan^{-1}(e^{-t}) - \frac{\pi}{2} \right)$$

This characterization brings us to our second main result of this section.

Theorem 4.5. *The action of U_- on $\dot{f}_0$ can be represented exactly by the following integral formula:*

$$U_- \dot{f}_0 = \int_{-\infty}^{0} e^t\, U_- \left[(X_\perp \pi^* \psi)\, (V f_0) \right] (\varphi_t(x, y, \theta))\; dt. \tag{17}$$

Proof. We begin by applying Lemma 2.18:

$$\begin{aligned} [X,\, U_-]\dot{f}_0 = -U_- \dot{f}_0 \quad &\Longrightarrow \quad X(U_- \dot{f}_0) - U_-(X \dot{f}_0) = -U_- \dot{f}_0 \\ &\Longrightarrow \quad (X + 1)(U_- \dot{f}_0) = U_-(X \dot{f}_0). \end{aligned}$$

Let us define $h := U_-(X \dot{f}_0)$. Then $U_- \dot{f}_0$ satisfies the same inhomogeneous transport equation $(X + 1)U_- \dot{f}_0 = h$ as considered in Lemma 4.3. Consequently, we may apply the solution formula derived there, provided we adopt the reparameterization of the flow map from Definition 4.4 that allows us to integrate nicely from $-\infty$ to 0.

This process yields

$$\begin{aligned} U_- \dot{f}_0 = \int_{-\infty}^{0} e^t\, h(\varphi_t(x, y, \theta))\, dt &= \int_{-\infty}^{0} e^t\, (U_- X \dot{f}_0)(\varphi_t(x, y, \theta))\, dt \\ &= \int_{-\infty}^{0} e^t\, U_- \left[(X_\perp \pi^* \psi)\, (V f_0) \right] (\varphi_t(x, y, \theta))\, dt, \end{aligned}$$

where the substitution $X \dot{f}_0 = (X_\perp \pi^* \psi)\, (V f_0)$ follows directly from Theorem 4.2. ∎

5 Fourier analysis of $\dot{f}_0$

To analyze the fine structure of $\dot{f}_0$, write its kth Fourier modes (including the $e^{ik\theta}$ factor) as

$$\dot{f}_0(\theta) = \sum_{k \in \mathbb{Z}} \dot{f}_0^{(k)}(\theta), \quad X \dot{f}_0(\theta) = \sum_{k \in \mathbb{Z}} \ell^{(k)}(\theta), \quad U_- \dot{f}_0(\theta) = \sum_{k \in \mathbb{Z}} m^{(k)}(\theta),$$

where

$$\dot{f}_0^{(k)}(\theta) = f_k\, e^{ik\theta}, \quad \ell^{(k)}(\theta) = \ell_k\, e^{ik\theta}, \quad m^{(k)}(\theta) = m_k\, e^{ik\theta}.$$

Since $V = \partial_\theta$ acts by $V(e^{ik\theta}) = ik\, e^{ik\theta}$, each exponential is an eigenfunction and V acts diagonally on these modes.

Theorem 5.1. *The two principal Fourier modes of $\dot{f}_0$ are given by:*

$$\dot{f}_0^{(1)} = i\, m_1 + \ell_1 - 2\,\eta_+\, \dot{f}_0^{(0)} \quad \textit{and} \quad \dot{f}_0^{(-1)} = -i\, m_{-1} + \ell_{-1} - 2\,\eta_-\, \dot{f}_0^{(0)},$$

where

$$\dot{f}_0^{(0)}(z) = 2\int_{\Gamma\backslash\mathbb{H}} G(z,w)\,\phi(w)\,dA(w) \quad \textit{and} \quad \phi := \frac{\ell^{(0)} + i\, m^{(0)}}{2} + i\,\eta_+\, m^{(-1)} - \eta_+\, \ell^{(-1)}.$$

Proof. It follows immediately from Definition 2.16 that

$$X = \eta_+ + \eta_-, \qquad U_- = X_\perp - V = \frac{1}{i}(\eta_+ - \eta_-) - V.$$

Next, we compute

$$\sum_{k\in\mathbb{Z}} \ell^{(k)} = X\dot{f}_0 = \sum_k (\eta_+ + \eta_-)\big(\dot{f}_0^{(k)}\big) = \sum_k \big(\eta_+\, \dot{f}_0^{(k-1)} + \eta_-\, \dot{f}_0^{(k+1)}\big);$$
$$\sum_{k\in\mathbb{Z}} m^{(k)} = U_-\dot{f}_0 = \sum_k \Big[\tfrac{1}{i}(\eta_+ - \eta_-)\big(\dot{f}_0^{(k)}\big) - V\big(\dot{f}_0^{(k)}\big)\Big] = \sum_k -i\big(k\, \dot{f}_0^{(k)} - \eta_-\, \dot{f}_0^{(k+1)} + \eta_+\, \dot{f}_0^{(k-1)}\big).$$

Since the exponentials $e^{ik\theta}$ are linearly independent (indeed orthogonal), the coefficient of each $e^{ik\theta}$ in the two sums must coincide. Hence we attain explicit expressions for the modes of $X\dot{f}_0$ and $U_-\dot{f}_0$ in terms of the modes of $\dot{f}_0$:

$$\ell^{(k)} = \eta_+\, \dot{f}_0^{(k-1)} + \eta_-\, \dot{f}_0^{(k+1)}; \quad m^{(k)} = -i\big(k\, \dot{f}_0^{(k)} - \eta_-\, \dot{f}_0^{(k+1)} + \eta_+\, \dot{f}_0^{(k-1)}\big).$$

Setting $k = 1$ into both relations, we see that $\ell^{(1)} = \eta_+\, \dot{f}_0^{(0)} + \eta_-\, \dot{f}_0^{(2)}$ and $m^{(1)} = -i\big(\dot{f}_0^{(1)} - \eta_-\, \dot{f}_0^{(2)} + \eta_+\, \dot{f}_0^{(0)}\big)$. The first equation tells us that $\eta_-\, \dot{f}_0^{(2)} = \ell^{(1)} - \eta_+\, \dot{f}_0^{(0)}$, and substituting for this term in the second yields

$$m^{(1)} = -i\Big(\dot{f}_0^{(1)} - (\ell^{(1)} - \eta_+\, \dot{f}_0^{(0)}) + \eta_+\, \dot{f}_0^{(0)}\Big) = -i\big(\dot{f}_0^{(1)} - \ell^{(1)} + 2\eta_+\, \dot{f}_0^{(0)}\big).$$

Rearranging gives

$$\dot{f}_0^{(1)} = i\, m^{(1)} + \ell^{(1)} - 2\,\eta_+\, \dot{f}_0^{(0)}. \tag{18}$$

An identical process can be carried out by setting $k = -1$ in both relations, leading to the explicit expression

$$\dot{f}_0^{(-1)} = -\,i\, m^{(-1)} + \ell^{(-1)} - 2\,\eta_-\, \dot{f}_0^{(0)}. \tag{19}$$

The problem now reduces to solving for $f_0^{(0)}$. Setting $k = 0$ in the modal relations involving $\ell^{(k)}$

and $m^{(k)}$, we obtain

$$\ell^{(0)} = \eta_+ \dot{f}_0^{(-1)} \;+\; \eta_- \dot{f}_0^{(1)} \quad \text{and} \quad m^{(0)} = -i\big(0 \cdot \dot{f}_0^{(0)} - \eta_- \dot{f}_0^{(1)} + \eta_+ \dot{f}_0^{(-1)}\big) = i\,\eta_- \dot{f}_0^{(1)} - i\,\eta_+ \dot{f}_0^{(-1)}.$$

Solving this system for the "shifted" modes gives

$$\Big(\eta_+ \dot{f}_0^{(-1)},\, \eta_- \dot{f}_0^{(1)}\Big) = \left(\frac{\ell^{(0)} + i\,m^{(0)}}{2},\, \frac{\ell^{(0)} - i\,m^{(0)}}{2}\right). \tag{20}$$

Next, apply η_+ to (19):

$$\begin{aligned}
&\eta_+ \dot{f}_0^{(-1)} = -\,i\,\eta_+\, m^{(-1)} + \eta_+\, \ell^{(-1)} - 2\,\eta_+\eta_-\, \dot{f}_0^{(0)} \\
\implies\quad &\eta_+\eta_-\, \dot{f}_0^{(0)} = \tfrac{1}{2}\left(-\eta_+ \dot{f}_0^{(-1)} - \,i\,\eta_+\, m^{(-1)} + \eta_+\, \ell^{(-1)}\right) \\
\implies\quad &\eta_+\eta_-\, \dot{f}_0^{(0)} = -\tfrac{1}{2}\left(\frac{\ell^{(0)} + i\,m^{(0)}}{2} + \,i\,\eta_+\, m^{(-1)} - \eta_+\, \ell^{(-1)}\right),
\end{aligned}$$

where the substitution in the last step comes from (20).

To solve for $\dot{f}_0^{(0)}$, we aim to invert the operator $\eta_+\eta_- = -\frac{1}{4}\Delta_{\text{hyp}}$, the hyperbolic Laplacian on $\mathbb{H}$. Thus, inverting $\eta_+\eta_-$ amounts to solving a Poisson equation on the quotient space $\Gamma\backslash\mathbb{H}$. Define

$$\phi := \frac{\ell^{(0)} + i\,m^{(0)}}{2} + \,i\,\eta_+\, m^{(-1)} - \eta_+\, \ell^{(-1)},$$

which results in $\eta_+\eta_- \dot{f}_0^{(0)} = -\frac{1}{2}\phi$, or equivalently, $\Delta_{\text{hyp}} \dot{f}_0^{(0)} = 2\phi$. The unique solution can be written using the normalized Green's function $G(z,w)$ on $\Gamma\backslash\mathbb{H}$:

$$\dot{f}_0^{(0)}(z) = 2\int_{\Gamma\backslash\mathbb{H}} G(z,w)\,\phi(w)\,dA(w),$$

where $\Delta_z G(z,w) = \delta_w(z) - \frac{1}{\text{Vol}(\Gamma\backslash\mathbb{H})}$ and $dA(w) = \frac{dx\,dy}{y^2}$ denotes the hyperbolic area element. ■

6 Conclusion

Our work helps to verify new cases of the Fried conjecture by reducing the error in the expansion of $\zeta_R(s)$ near zero to the order of ε^2, providing more precise control when measuring how analytic torsion changes under metric perturbations. More broadly, these results clarify how subtle changes in the local geometry of a surface alter the way particles would classically move along geodesics and, in turn, shift the quantum signatures those trajectories leave behind. By showing how tightly classical motion and quantum behavior are linked, this work contributes to the broader effort to decode how deterministic systems produce the unpredictable patterns observed in quantum systems.

7 Acknowledgements

I would like to acknowledge the efforts of my mentor, Alain Kangabire, Dr. Tanya Khovanova, Prof. Roman Bezrukavnikov, and Dr. Jonathan Bloom for suggesting the problem and guiding the research process. I am also indebted to my tutor AnaMaria Perez as well as TAs Varun Thvar, Austin Luo, and Aditya Sood for their invaluable advice and support. Additionally, I would like to thank the Center for Excellence in Education, MIT, and Citadel Securities for hosting and sponsoring me this summer.

Last but certainly not least, I am endlessly grateful to my parents for their unwavering support—dnone of this would have been possible without their sacrifices.

References

[1] S. Dyatlov and M. Zworski. Dynamical zeta functions for anosov flows via microlocal analysis. *Annales scientifiques de l'École normale supérieure*, 49:543–577, 2016.

[2] S. Dyatlov and M. Zworski. Ruelle zeta function at zero for surfaces. *Inventiones Mathematicae*, 210(1):211–229, 2017.

[3] D. Fried. Fuchsian groups and reidemeister torsion. In D. A. Hejhal, P. Sarnak, and A. M. Weinstein, editors, *The Selberg trace formula and related topics*, volume 53 of *Contemporary Mathematics*, pages 141–163. American Mathematical Society, Providence, RI, 1986. Conference held in Brunswick, Maine, 1984.

[4] T. Medved. Dynamical torsion for surfaces of constant negative curvature. Unpublished manuscript, under the direction of Alain Kangabire, Research Science Institute, July 2024.

[5] S. Dyatlov. Notes on hyperbolic dynamics, 2018.

[6] C. Kogler. Closed geodesics on compact hyperbolic surfaces. `http://constantinkogler.com/Files/ConstantinKoglerBachelorThesis.pdf`, 2018. Bachelor's thesis, supervised by Prof. Dr. Marc Burger. [Accessed 15-07-2025].

[7] T. Fisher. Hyperbolic geodesic flow* — EMS Press — ems.press. `https://ems.press/content/book-chapter-files/22279`, 2019. [Accessed 03-07-2025].

[8] S. Dyatlov. Pollicott-ruelle resolvent and sobolev regularity. *Pure and Applied Functional Analysis*, 8(1):187–213, 2023.